JOURNAL OF MATERIALS SCIENCE **36** (2001) 5543–5550

Scanning electron microscope investigations of highly conducting organic composites

M. GOLUB, L. SZCZESNIAK
Institute of Molecular Physics, Polish Academy of Sciences, 60-179 Poznan, Poland

A. GRAJA
Institute of Molecular Physics, Polish Academy of Sciences, 60-179 Poznan, Poland; L.P.M.C., Université de Nice - Sophia Antipolis, 06108 Nice Cedex, France

A. BRAU, J.-P. FARGES
L.P.M.C., Université de Nice - Sophia Antipolis, 06108 Nice Cedex, France

Scanning electron microscope (SEM) investigation of the highly conducting organic composites of general formulae (BEDT-TTF)$_x$/(AuI) and (BEDT-TTF)$_x$/(AuI$_3$), where BEDT-TTF is bis(ethylenedithio)tetrathiafulvalene, obtained by direct charge-transfer (CT) reaction in the solid state is performed. The granular structure of the composites with domination of three types of the grains: (BEDT-TTF)$_2$I$_3$, (BEDT-TTF)$_2$AuI$_2$ and Au, is suggested. The changes in the composite structure caused by their composition and/or thermal treatment are connected with the d.c. electrical conductivity of the samples.

1. Introduction

Organic charge-transfer (CT) complexes, either semiconducting, metal-like or superconducting, based on bis(ethylenedithio)tetrathiafulvalene (BEDT-TTF) are most commonly obtainable in the form of tiny single crystals with submillimeter dimensions [1–4]. These conducting crystals are not of great practical interest because they are very small and brittle. There have been various attempts to obtain organic conducting materials in form more suitable for applications e.g. reticulate doping of polymeric films [5], evaporation of thin conducting films [6], fabrication of polycrystalline samples [7] or preparation of conducting composite materials by the way of a CT reaction produced directly in the solid state between organic electron donor and acceptor molecules [8–10]. This last possibility was already established in the past for TTF as the donor and a variety of solid acceptors. The CT reaction is occurring by grinding together two components of various electron properties [8, 10]. Numerous conducting composite samples showing metallic behaviors, with good mechanical properties and almost unlimited size, have so been obtained under appropriate mechanical and thermal treatments [8–14].

Although the electrical transport and optical properties of organic conducting composites obtained by direct CT reaction in the solid state are rather well known, their structure should be better investigated. In this paper we report results of scanning electron microscope (SEM) imaging of the composites of BEDT-TTF with two compounds AuI and AuI$_3$ of various compositions and thermal treatments. The general formulae of the investigated composites are: (BEDT-TTF)$_x$/(AuI) and (BEDT-TTF)$_x$/(AuI$_3$), where x is the molar ratio of acceptor to donor molecules. Observed changes in the composite structure are discussed in relation with the electrical conductivity of the samples.

2. Experimental

Each composite sample is prepared according to a general procedure described in previous papers [8–13]. Defined proportions of solid donor (BEDT-TTF) and solid acceptor (AuI or AuI$_3$) are ground together for 8 hours, at room temperature. The resulting powdered mixture is then compacted under 5 kbar pressure in the form of disk. The samples prepared in this way are then annealed at temperature and for time experimentally chosen so as to get the highest d.c. electrical conductivity.

For the d.c. electrical conductivity measurements the samples are put in the form of bars on which gold contacts are evaporated in four-probe geometry. Silver wires are then stuck to these contacts with silver paint. The conductivity is measured between room temperature and 4 K using Keithley 182 sensitive digital voltmeter and Keithley 220 programmable current source. The continuous flow helium cryostat Optistat CF with temperature controller ITC 503 made by Oxford Instruments is used for temperature stabilization. The conductivity is determined from the slope of the V–I characteristics for four currents. This method not only eliminates an offset voltage but also automatically checks that the applied current is not enough to heat sample and is in the linear region of V–I characteristics.

The highest electrical conductivity value is researched for each composite material, requiring first a careful determination of the following parameters to be optimized separately: the proportion of the two

components in the mixture, given here by x, the time of mechanical grinding as well as the time and temperature of annealing. The optimal x-value so obtained, corresponding to a conductivity maximum of the sample, reaches 11 $S \cdot cm^{-1}$ in $(BEDT\text{-}TTF)_x(AuI)$ samples and 8 $S \cdot cm^{-1}$ in $(BEDT\text{-}TTF)_x(AuI_3)$, at room temperature.

TESLA scanning electron microscope BS 300 is used for investigation of the surface structure of the composite samples. The accelerating voltage of 15 kV and observation in secondary electron mode are applied. Micrographs from this mode are nearly the same as obtained in back scattering mode. The pictures are taken at SEM magnifications of 2000 and 5000. Because of their high electrical conductivity the samples can be investigated by SEM without preliminary preparation of the surface. It has to be noticed that in some cases microcrystals in the composite samples are influenced by electron beam and the picture changes during observation.

3. SEM imaging of conducting composites

3.1. Morphology of the composite

Morphology of the surface of the conducting organic composite samples depends on their composition, way of preparation and annealing conditions. The same factors determine of course the electrical transport and

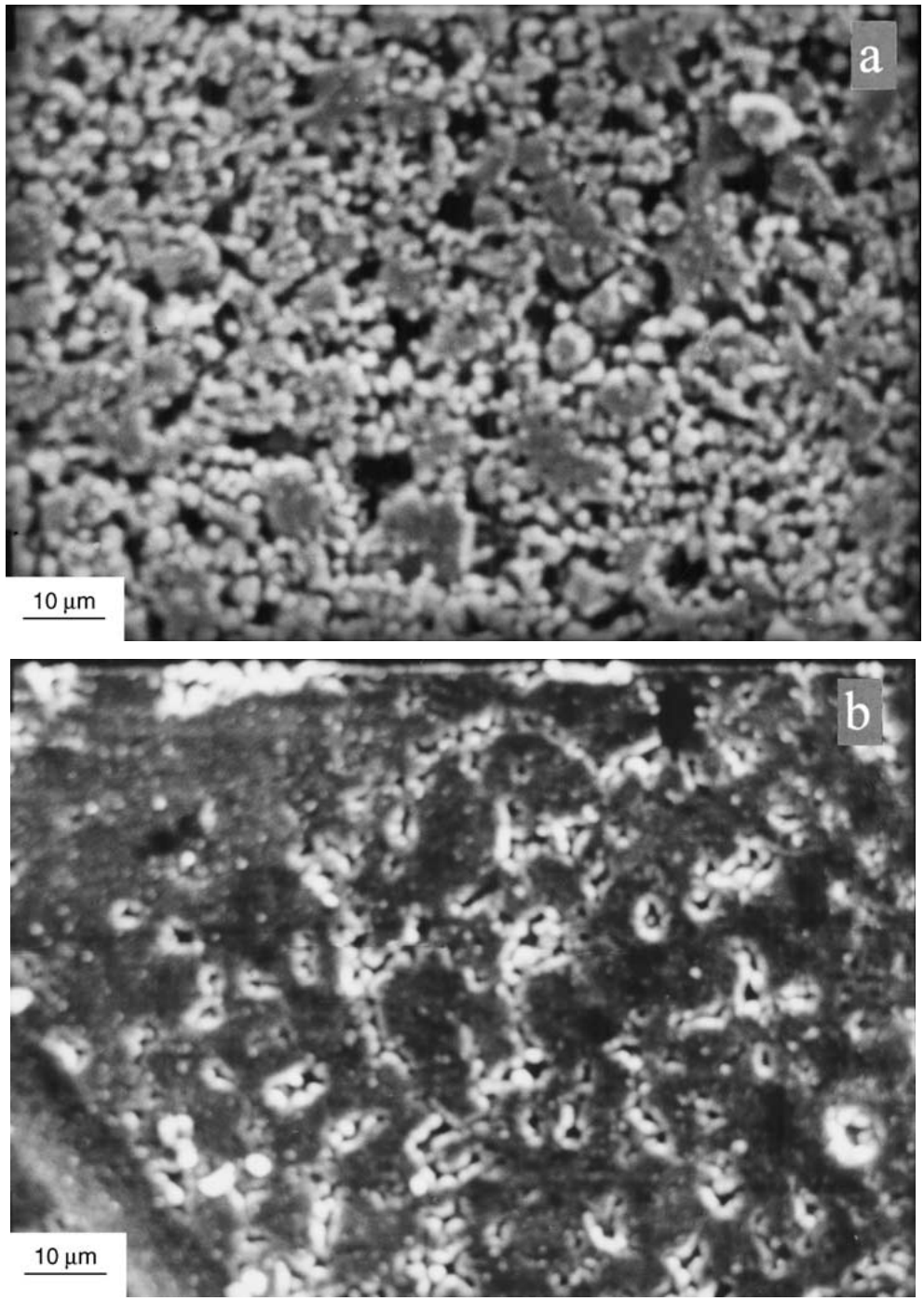

Figure 1 Typical SEM micrographs of the surfaces of the $(BEDT\text{-}TTF)_x$/(AuI) samples before annealing with $x = 0.82$ (a) and after annealing with $x = 0.5$, 0.82 and 1.5 (b, c and d). (*Continued*.)

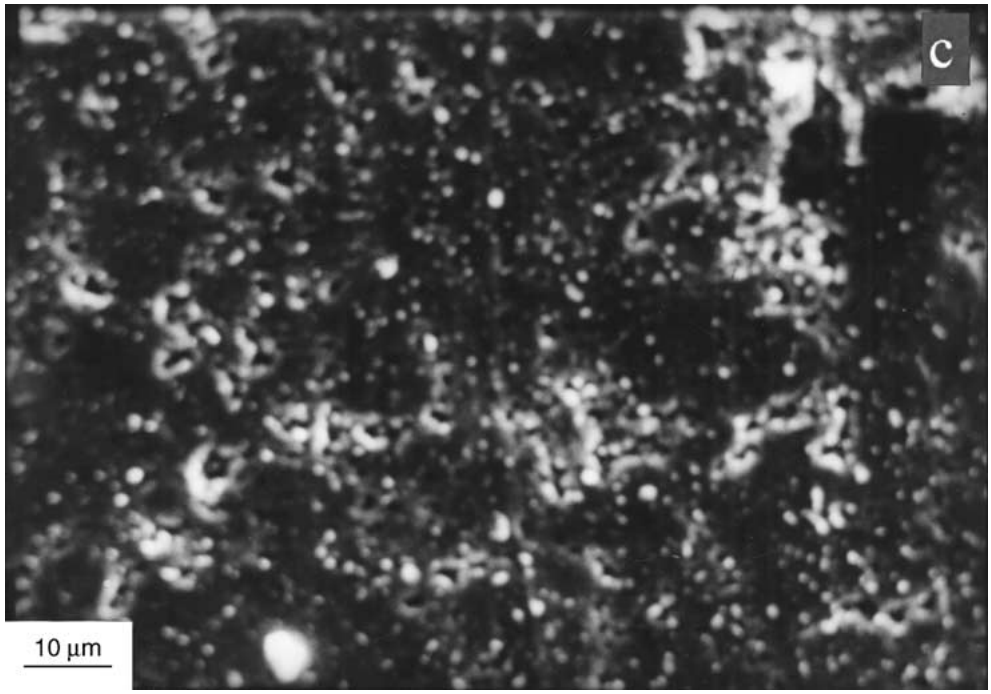

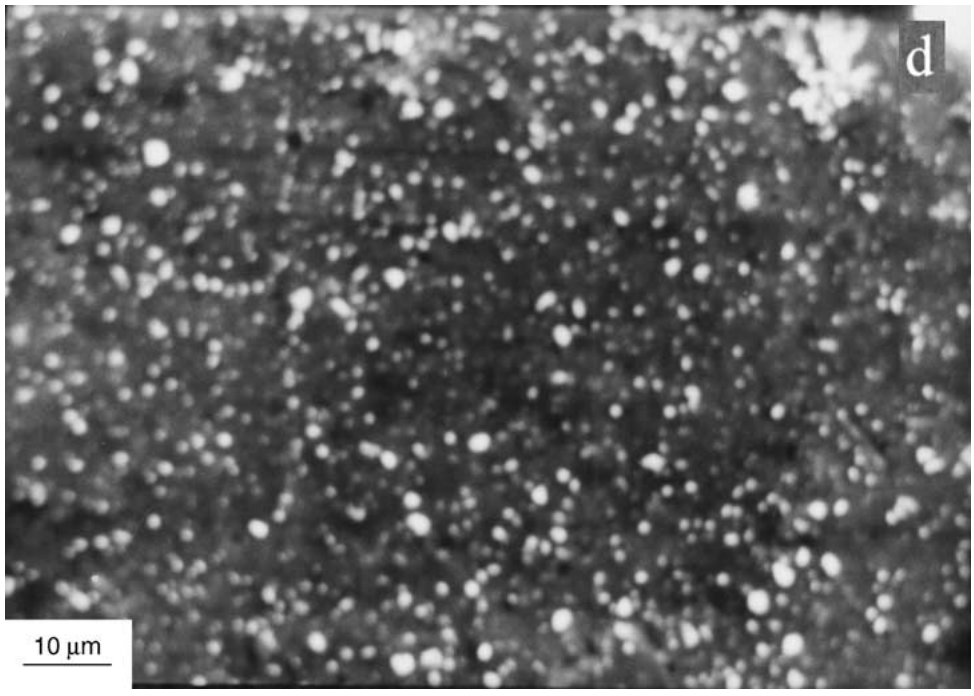

Figure 1 (*Continued.*)

optical properties of the samples. Thus the study of the internal structure and of the morphology of the composites in relation with their physical properties is of interest.

Typical SEM micrographs of surfaces of the (BEDT-TTF)$_x$/(AuI) samples, for $x = 0.5$, 0.82 and 1.5 are shown in Fig. 1 and for (BEDT-TTF)$_x$/(AuI_3) with $x = 1.0$, 1.5 and 2.17 in Fig. 2. Voids and grains of various dimensions and forms are observed as a result of the heterogeneous character of the composites. The composite surface morphology reminds the texture of a sponge. The chemical composition of the grains seems to be different also from sample to sample. It has been shown recently from X-ray diffractograms and Raman spectra, that (BEDT-TTF)$_x$/(AuI) and (BEDT-TTF)$_x$/(AuI_3) composite samples are mainly composed of (BEDT-TTF)$_2I_3$ and (BEDT-TTF)$_2AuI_2$ grains [15], together with neutral gold. This can be expressed schematically by the following formulae:

$$4\,(\text{BEDT-TTF}) + 5\,\text{AuI} \rightarrow (\text{BEDT-TTF})_2\text{I}_3 + (\text{BEDT-TTF})_2\text{AuI}_2 + 4\,\text{Au}$$

$$4\,(\text{BEDT-TTF}) + 2\,\text{AuI}_3 \rightarrow (\text{BEDT-TTF})_2\text{I}_3 + (\text{BEDT-TTF})_2\text{AuI}_2 + \text{Au} + 1/2\,\text{I}_2$$

This corresponds to a donor to acceptor molecular ratio of $x_{cal} = 0.8$ for (BEDT-TTF)$_x$/(AuI) and of $x_{cal} = 2.0$ for (BEDT-TTF)$_x$/(AuI_3) samples. These values well correspond also with the composite

sample compositions experimentally found to have a conductivity maximum: $x_{exp} = 0.82$ and $x_{exp} = 2.0$, respectively [15]. The grains (BEDT-TTF)$_2$I$_3$ and (BEDT-TTF)$_2$AuI$_2$ are difficult to distinguish by SEM. However, preliminary X-ray microanalysis (XMA) investigations show areas with different iodine contents, suggesting existence for both types of grains. XMA shows also that free gold is present in the composites [16]. According to this the clear, light, small spots visible in the SEM images could be Au grains.

The SEM micrographs of (BEDT-TTF)$_x$/(AuI) show that such the samples are more heterogeneous and with more voids between grains before annealing (Fig. 1a) than after (Fig. 1c). The samples were annealed at temperatures between 80°C and 155°C; so that iodine, AuI and AuI$_3$ can melt or even decompose and can diffuse into the bulk of the BEDT-TTF component helping formation of the CT complexes. This effect results also in an increase of the d.c. electrical conductivity of annealed samples [15]. It is possible that some form of recrystallization occurs during the annealing. Some molecular ordering of the (BEDT-TTF)$_x$/(AuI) and (BEDT-TTF)$_x$/(AuI$_3$) composites have been detected by X-ray analysis [15]. It is possible also that gold grains formed under sample annealing influence its electrical conductivity. The sample porosity apparently decreases also with an increase of BEDT-TTF contents (Fig. 1b, c and d); the sample with an excess of BEDT-TTF (Fig. 1d) shows rather small porosity. In this case intergrain voids are better filled with

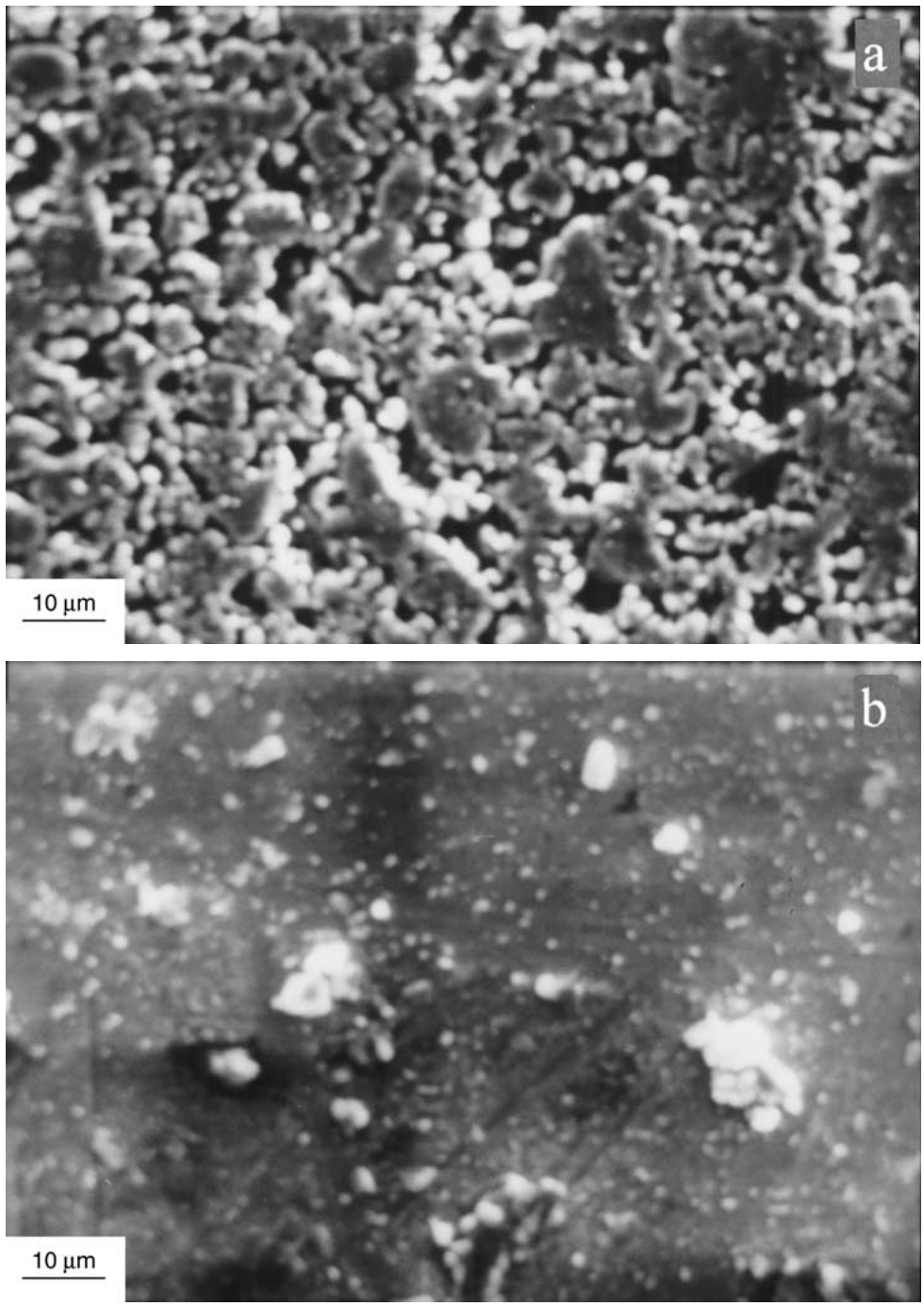

Figure 2 Typical SEM micrographs of the surfaces of the (BEDT-TTF)$_x$/(AuI$_3$) samples before annealing with $x = 1.5$ (a) and after annealing with $x = 1.0$, 1.5 and 2.17 (b, c and d). (*Continued*.)

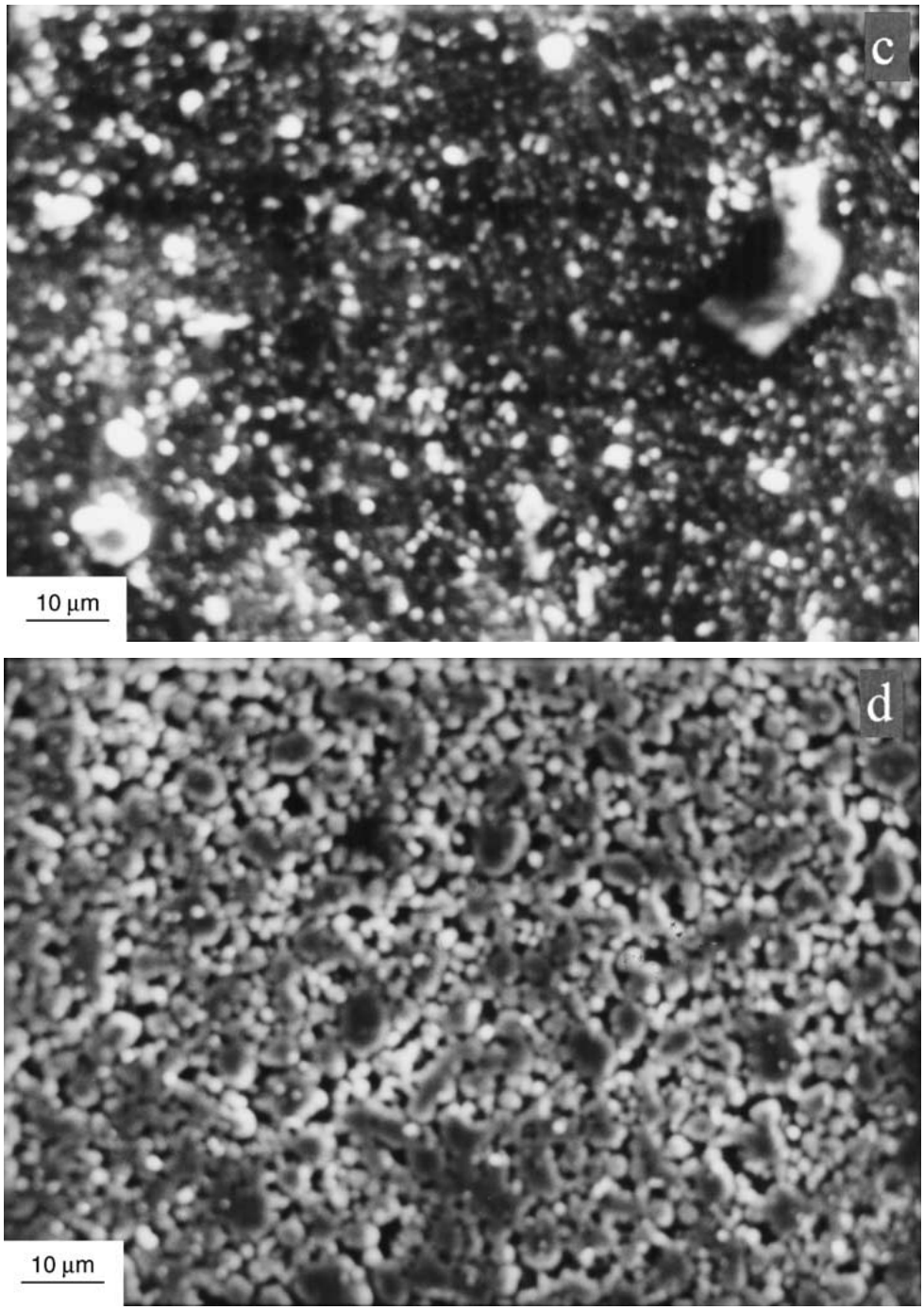

Figure 2 (*Continued*.)

non-bounded acceptor molecules. It is also possible that some amorphous products of the solid state CT reaction fill in the voids. On the other hand the number of bright spots, which could be attributed to Au grains, is maximal for $(BEDT\text{-}TTF)_{0.82}/(AuI)$. This is consistent with the highest conductivity of this sample and corresponds to the maximum of CT reaction output.

An analysis of the SEM micrographs of $(BEDT\text{-}TTF)_x/(AuI_3)$ (Fig. 2) is more complicated. The inter-grain voids fill in and the sample porosity decreases with sample annealing (Fig. 2a and c) but it seems that the porosity is not only a function of BEDT-TTF contents in the mixture (Fig. 2b, c and d). On the other hand, the d.c. electrical conductivity increases from 0.09 $S \cdot cm^{-1}$ for $(BEDT\text{-}TTF)/(AuI_3)$ to 8.04 $S \cdot cm^{-1}$ for $(BEDT\text{-}TTF)_{2.17}/(AuI_3)$ in correspondence with an increase of the number of bright spots in the SEM image.

3.2. Heterogeneity of the composites

The annealing may not be uniform within the bulk of the composite samples. The structural sample heterogeneity induced by this effect can be observed by the SEM method. Fig. 3 shows micrographs of a fracture in a $(BEDT\text{-}TTF)_{0.82}/(AuI)$ sample before (Fig. 3a) and after (Fig. 3b and c) annealing. The latter micrographs show the structures of areas of the same broken sample but differently modified due to temperature gradients in the sample. The morphology of the fracture is that of layered or fibrous structures for all investigated

composites. However, Fig. 3 shows that details of these structures can be different. The morphology of the area shown in Fig. 3b is nearly the same as that of the sample before annealing (Fig. 3a); whereas the morphology of the area shown in Fig. 3c is different. This region of material shows a well developed layered structure, smaller porosity and probably higher electrical conductivity. A similar effect can be observed for pressed samples with density gradient. Effects mentioned above could explain atypical temperature dependence of the electrical conductivity of some samples.

3.3. Role of sample ageing

Ageing of composite samples produces strong irreversible modifications of electrical transport properties. This is shown in Fig. 4 where the temperature dependence of the d.c. electrical conductivity of (BEDT-TTF)$_{2.17}$/(AuI_3) composite samples before and after annealing are shown. The properties of the sample annealed for about one day after preparation ("fresh") are shown in Fig. 4a. The annealing at $T = 80°C$ during 2 hours causes a change in the transport properties, from semiconducting (black circles) to metal-like behavior (open circles), together with significant increase of the room temperature conductivity. The conductivity increases slowly, as temperature decreases, up to a maximum at about 45–50 K and then it decreases like a thermally activated semiconductor. The temperature dependent d.c. electrical conductivity of the sample can be approximated by Epstein's *et al*. [17] equation:

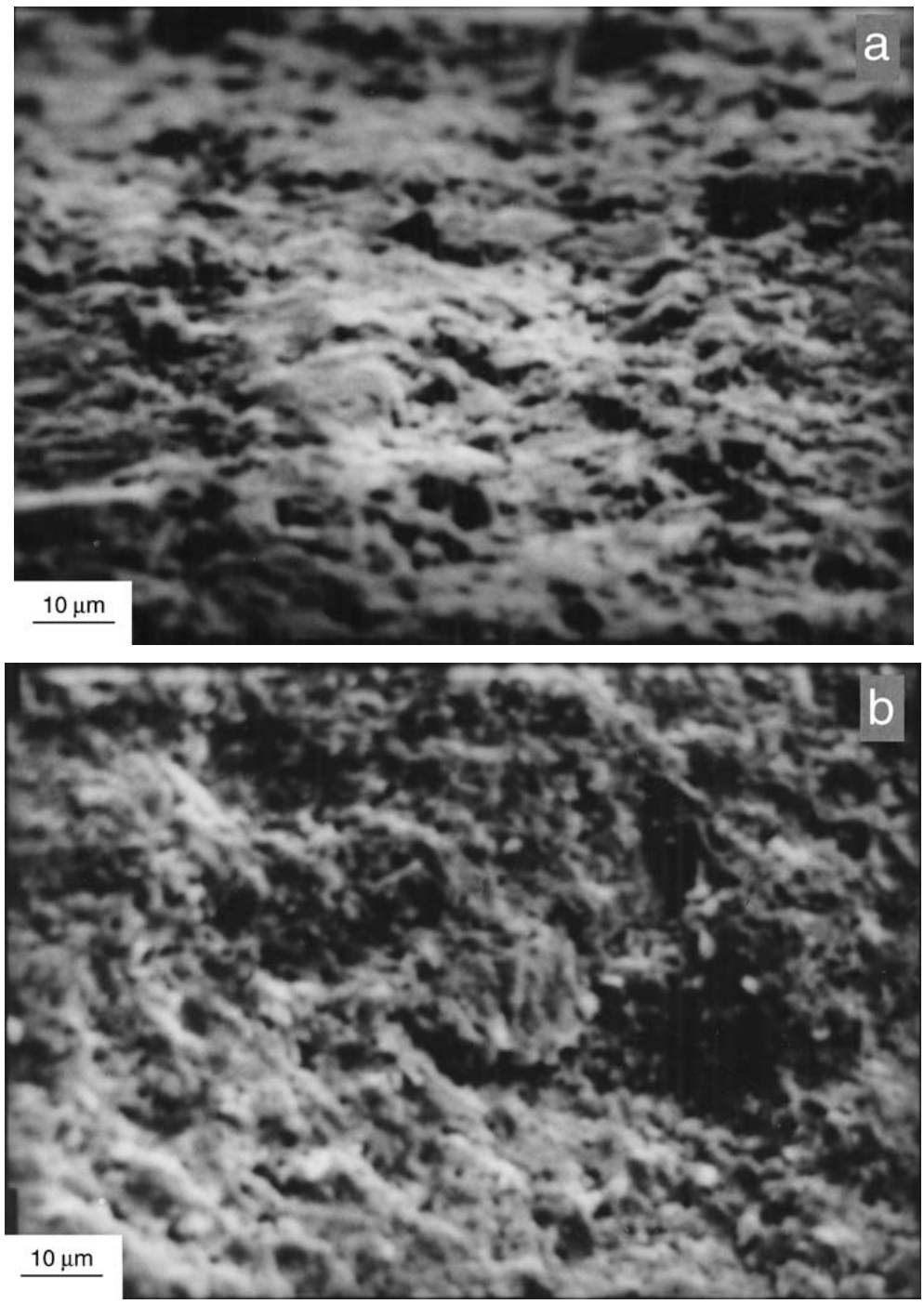

Figure 3 Micrographs of the break of the (BEDT-TTF)$_{0.82}$/(AuI) sample before (a) and after (b and c) annealing. (*Continued*.)

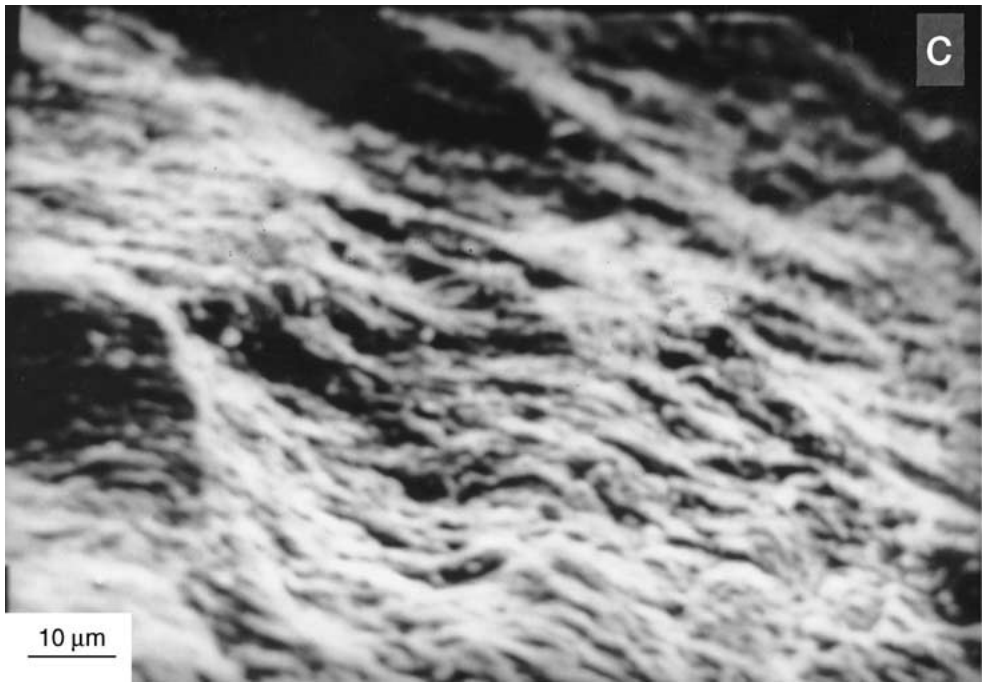

Figure 3 (*Continued.*)

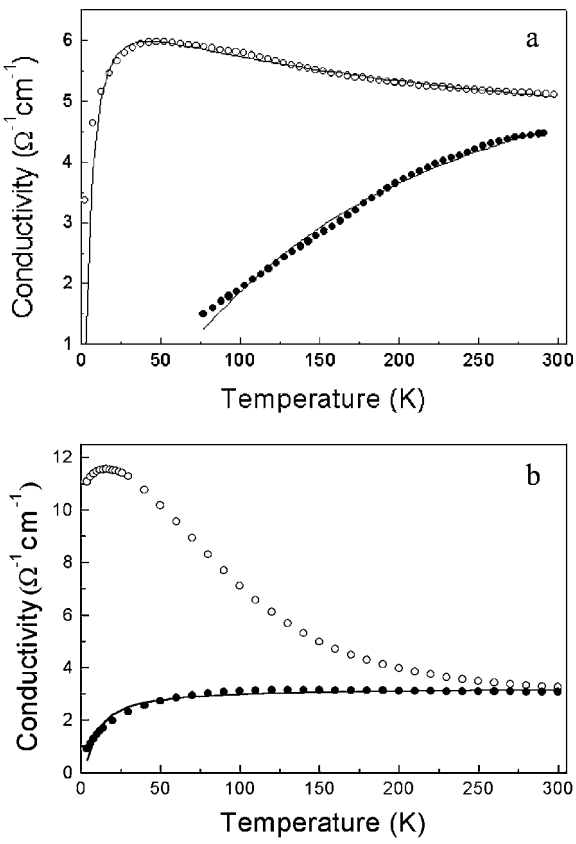

Figure 4 Temperature dependence of the d.c. electrical conductivity of "fresh" (a) and "old" (b) samples of $(BEDT\text{-}TTF)_{2.17}/(AuI_3)$ composite before and after annealing. The time and temperature of annealing are: 2 hour, 80°C for (a) and 54 hours, 85°C for (b), respectively. The solid lines show the best fits to Epstein's equation with parameters given in the text.

$$\sigma(T) = AT^{-\alpha} \exp(-\Delta/T)$$

where Δ is an apparent activation energy, a prefactor $T^{-\alpha}$ shows a large strongly temperature-dependent mobility of charge carriers, $\mu(T)$ and A is a constant prefactor. The best fits with $A = 7.16$, $\alpha = 0$ and $\Delta = 134.5$ K, for the sample before annealing and with $A = 12.3$, $\alpha = 0.15$ and $\Delta = 6.4$ K, for the annealed sample, are shown in Fig. 4a as solid lines. Correspondence of the experimental data with the model confirms, that the "fresh" sample before annealing is a thermally activated semiconductor with a gap of about 11.6 meV, but the annealed sample becomes a metal-like material with very narrow gap of 0.55 meV and $\mu(T) \propto T^{-0.15}$.

Annealing of the sample prepared about 6 months earlier ("old") requires much longer times, up to 54 hours to reach a conductivity maximum and leads to inconsiderable increase of the room temperature conductivity (Fig. 4b). However, the conductivity increases much faster as temperature decreases, to a maximum at $T = 15$ K, where it decreases slowly. The conductivity of the "old" sample before annealing can be also fitted (Fig. 4b) with Epstein's formula with $A = 3.2$, $\alpha = 0$ and $\Delta = 7.6$ K; it means that the sample is still semiconducting with very small gap of 0.65 meV. It is interesting that the gap is only insensibly larger than the gap of the annealed "fresh" sample. The conductivity of annealed "old" sample cannot be described by Epstein's formula; it suggests that the conductivity is influenced by other mechanisms.

The above-mentioned differences are caused by various properties of "fresh" and "old" non-annealed samples. The CT reaction is not completed during mechanical treatment (grinding) in the former sample and only after annealing the reaction comes nearly to the end. As experiment shows, the short time of sample annealing (1–2 hours) is sufficient for the reaction to be completed. Thus, the annealed sample is transformed nearly entirely to metal-like phase. In the "old" sample the CT reaction is completing progressively during the time interval between the sample preparation and its annealing. It seems that a delay of about 6 months is required for the reaction to be completed. Therefore

the room temperature conductivity is not significantly changed after 1–2 hour annealing but it increases inconsiderably after an extremely long annealing time, e.g. 60 hours. However, the increase of the conductivity as temperature decreases is much stronger than in "fresh" sample. This effect shows a different nature. X-ray microanalysis has revealed considerable silver contents. The only possible explanation is diffusion of the silver paint used to fasten wires to evaporated gold electrodes. A silver diffusion from the paint to organic samples is postulated from ferroelectric crystals or fullerenes [18] investigations.

4. Conclusions

Contrary to (BEDT-TTF)$_2$/I$_3$ composite (BEDT-TTF)$_x$/(AuI) and (BEDT- TTF)$_x$/(AuI$_3$) composites are not superconducting. There are two reasons for electron localization in these materials: (1) a structural disorder introduced by the mechanochemical method of sample preparation and (2) a chemical disorder corresponding to the mixture of three phases: (BEDT-TTF)$_2$I$_3$, (BEDT-TTF)$_2$AuI$_2$ and Au as well as some unidentified amorphous phases. Generally speaking, the grain-like structure of composite samples is the main reason for metal to insulator transition in the investigated composites.

SEM investigation of both (BEDT-TTF)$_x$/(AuI) and (BEDT-TTF)$_x$/(AuI$_3$) composites gives evidence for strong similarities in their morphology; both show a granular structure with domination of three types of the grains. The structure becomes more dense after annealing and usually the composite porosity is also decreasing with increasing of the BEDT-TTF contents in the mixture.

References

1. J. M. WILLIAMS, J. R. FERRARO, R. J. THORN, K. D. CARLSON, U. GEISER, H. H. WANG, A. M. KINI and M.-H. WHANGBO, "Organic Superconductors (Including Fullerenes). Synthesis, Structure, Properties and Theory" (Prentice Hall, New Jersey, 1992).
2. A. GRAJA, "Low-Dimensional Organic Conductors" (World Scientific, Singapore, New Jersey, London, Hong Kong, 1992).
3. J.-P. FARGES (ed.), "Organic Conductors: Fundamentals and Applications" (Marcel Dekker, New York, 1994).
4. T. ISHIGURO, K. YAMAJI and G. SAITO, "Organic Superconductors" (Springer-Verlag, Berlin, Heidelberg, New York, 1998).
5. J. K. JESZKA, J. ULANSKI and M. KRYSZEWSKI, *Nature* **298** (1981) 390.
6. K. KAWABATA, K. TANAKA and M. MIZUTANI, *Solid State Commun.* **74** (1990) 83.
7. D. SCHWEITZER, P. BELE, H. BRUNNER, E. GOGU, U. HAEBERLEN, I. HENNING, T. KLUTZ, R. SWIETLIK and H. J. KELLER, *Z. Phys. B—Condensed Matter* **67** (1987) 489.
8. J. P. FARGES, A. BRAU and P. DUPUIS, *Solid State Commun.* **54** (1985) 531.
9. J. P. FARGES, A. BRAU and F. ALI SAHRAOUI, *Mol. Cryst. Liq. Cryst.* **186** (1990) 143.
10. J. P. FARGES and A. BRAU, in "Handbook of Advanced Electronic and Photonic Materials and Devices," edited by H. S. Nalwa (Academic Press, San Diego, 2001) p. 329.
11. I. SMIRANI, A. BRAU and J. P. FARGES, *Synth. Met.* **93** (1998) 203.
12. V. N. SEMKIN, A. GRAJA, I. SMIRANI, A. BRAU and J. P. FARGES, *J. Mol. Structure.* **511–512** (1999) 49.
13. A. BRAU, I. SMIRANI, J. P. FARGES, R. LIPIEC and A. GRAJA, *Synth. Met.* **108** (2000) 75.
14. A. GRAJA, A. BRAU and J. P. FARGES, *Synth. Met.* **122** (2001) 233.
15. A. GRAJA, A. BRAU, J. P. FARGES, M. GOLUB, A. TRACZ and J. K. JESZKA, *Synth. Met.* **120** (2001) 753.
16. M. GOLUB, A. GRAJA, A. BRAU and J. P. FARGES, *Synth. Met.* (accepted).
17. A. J. EPSTEIN, E. M. CONWELL and J. S. MILLER, in "Annals of the New York Academy of Sciences," Vol. 313, edited by J. S. Miller and A. J. Epstein (The New York Academy of Sciences, New York, 1978) p. 183.
18. A. ZAHAB, L. FIRLEJ, F. BROCARD and N. KIROVA, *Synth. Met.* **77** (1996) 59.

Received 9 March
and accepted 24 July 2001